International Journal of Modern Physics A

Strange hadron measurement in d+Au collisions at $\sqrt{s_{\rm NN}} = 200$ GeV at STAR

Ishu Aggarwal
for the STAR Collaboration

Department of Physics
Panjab University Chandigarh-India
ishugoyal979@gmail.com

Strangeness production has been suggested as a sensitive probe to the early dynamics of the deconfined matter created in heavy-ion collisions. Ratios of particle yields involving strange particles are often utilized to study freeze-out properties of the nuclear matter, such as the strangeness chemical potential and the chemical freeze-out temperature. d+Au data connect Au+Au and p+p collisions, and help us to gain insight on the strangeness enhancement in the deconfined matter. The study of nuclear modification factor in d+Au collisions can also help to understand cold nuclear matter effects.

In this work, we will present new measurements on the production of strange hadrons (${K_S}^0$, Λ, Ξ, Ω) at mid-rapidity in d+Au collisions at $\sqrt{s_{\rm NN}} = 200$ GeV, recorded by the STAR experiment in 2016. The physics implications of the measurement on the collision dynamics will be discussed.

Keywords: Heavy-ion collisions; QGP; RHIC; STAR.

1. Introduction

The primary goal of high-energy heavy-ion (A–A) collisions is to create a system of deconfined quarks and gluons, known as quark–gluon plasma (QGP), and to study its properties. The transverse momentum (p_T) distributions of the particles produced in high-energy nuclear collisions can provide insights into the nature of the produced hot and dense matter and its dynamical evolution.

Asymmetric collision systems like proton-nucleus (p–A) and deuteron-nucleus (d–A) can be considered as control experiments where the formation of an extended QGP phase is not expected. These collision systems are used as baseline measurements to study the possible effects of cold nuclear matter and disentangle them from hot dense matter effects present in heavy-ion collisions. Hadron production can be affected by various factors, including alterations in parton distribution functions within nuclei, the possiblity of parton saturation, multiple scatterings, and radial flow. It is anticipated that these effects may vary with the rapidity of the produced particles.

Strange hadrons are useful probes for identifying the phase boundary and onset of deconfinement. Strangeness enhancement in heavy-ion collisions with respect to p+p collisions has long been suggested as a signature of QGP formation. But creation of QGP in small systems is still under intense debate. Strangeness has been extensively measured in many experiments at different accelerator facilities. Generally, the yields of strange hadrons in nuclear collisions are close to those expected from statistical models. The precise measurement of these yields in heavy-ion colisions may lead to a better understanding of strangeness production mechanisms in nuclear collisions and a better insight into the chemical freeze-out parameters.

The mechanisms for particle production in d+Au collisions at RHIC may be different at forward and backward rapidities. The partons from the deuteron-side (forward rapidity) are expected to undergo multiple scattering while traversing the gold nucleus. Those on the gold-side (backward rapidity) are likely to be more affected during collision. Study of nuclear effects can be performed using various observables, like Nuclear Modification Factor and Rapidity Asymmetry. Nuclear modification factor is defined as the ratio of the yield of particle in heavy-ion collisions ($\mathrm{Y_{AB}}$) to its yield in proton-proton collisions ($\mathrm{Y_{pp}}$), scaled by the number of binary nucleon-nucleon inelastic collisions.

$$\mathrm{R_{AB}(p_T)} = \frac{\mathrm{Yield_{AB}}}{\langle \mathrm{N_{bin}} \rangle \mathrm{Yield_{pp}}} \tag{1}$$

where $\langle \mathrm{N_{bin}} \rangle$ is the average number of binary nucleon-nucleon collisions.

Comparative study of particle production in forward and backward rapidity regions is done using rapidity asymmtery ($\mathrm{Y_{Asym}}$). $\mathrm{Y_{Asym}}$ is defined as

$$\mathrm{Y_{Asym}(p_T)} = \frac{\mathrm{Y_B(p_T)}}{\mathrm{Y_F(p_T)}} \tag{2}$$

where $\mathrm{Y_B}$ and $\mathrm{Y_F}$ are backward and forward particle yields, respectively. $\mathrm{Y_{Asym}}$ may provide unique information to help determine the relative contributions of various physics processes affecting particle production, such as multiple scattering, nuclear shadowing, recombination of thermal partons, and parton saturation.

2. Experimental Setup

The STAR is a versatile particle detector at the RHIC collider at Brookhaven National Laboratory. A detailed description of its solenoidal magnet and various subdetectors for tracking, particle identification, and triggering can be found in Ref. [1].

The TPC is STAR's primary tracking device. It is 4.2m long and 4m in diameter. The sensitive volume of the TPC contains P10 gas (10% methane, 90% argon) regulated at 2mbar above atmospheric pressure. The TPC data are used to determine particle trajectories, momenta, and particle-type through ionization energy loss (dE/dx). Its acceptance covers pseudorapidity (-1.8 $< \eta <$ 1.8) and the full azimuthal angle (2π). The track of a charged particle can be reconstructed with a maximum of 45 hit points within the TPC fiducial radius of 0.5 $<$ r $<$ 2 m. The location of the primary vertex of a collision event is determined using the reconstructed charged particle tracks. A primary vertex resolution in the transverse plane of 350 μm can be achieved with approximately 1000 tracks. The fitted primary vertex can be included in the track fitting of the charged particles to improve their momentum resolution. The TPC also measures the energy loss of charged particles, which allows separation of π and K to p_T approx. 0.7 GeV/c and identification of proton p_T approx. 1.1GeV/c.

3. Analysis Technique

A successful run of d+Au collisions at $\sqrt{s_{\mathrm{NN}}} = 200$ GeV was carried out in 2016 at RHIC. Total of approximately 100 million good events have been selected. The strange hadrons, $\mathrm{K^0_S}$, Λ, Ξ, Ω are identified and analyzed. These particles usually decay before they enter into the inner radius of Time Projection Chamber (TPC), so their decay products enter the TPC. STAR's tracking software is utilized to reconstruct the trajectories of daughters' tracks.

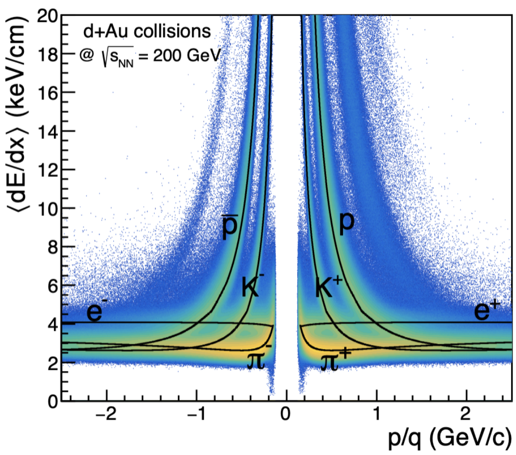

Fig. 1. The ⟨dE/dx⟩ of charged tracks is plotted as function of rigidity (p/q) in d+Au collisions at $\sqrt{s_{NN}} = 200$ GeV. The various bands correspond to different particles such as π, K, p. The curves represent the Bichsel expectation values of the corresponding particles.

Particle identification is accomplished by the energy loss (dE/dx) information measured by the TPC. Fig. 1 shows the average dE/dx of measured charged particles plotted as a function of "rigidity" (i.e., momentum/charge) of the particles. The curves represent the Bichsel expectation values. It can be seen that the TPC can identify pions, kaons, and protons at low momenta.

Strange hadrons can be reconstructed using invariant mass technique. K^0_S and Λ (generally referred to as $\mathrm{V^0}$) hadrons are reconstructed via their decay topology from their daughter particles. Decay channels are

$$\mathrm{K^0_S} \rightarrow \pi^+ + \pi^-,\ \text{Branch ratio } = (69.20 \pm 0.05)\% \tag{3}$$

$$\Lambda(\bar{\Lambda}) \rightarrow \mathrm{p}(\bar{\mathrm{p}}) + \pi^-(\pi^+),\ \text{Branch ratio } = (63.7 \pm 0.5)\% \tag{4}$$

while for Ξ and Ω baryon reconstruction, previously reconstructed Λ is combined with an additional charged track. This charged track is assumed to be pion(kaon) in $\Xi(\Omega)$ reconstruction. Decay channels of multi-strange hyperons are

$$\Xi^-(\bar{\Xi}^+) \rightarrow \Lambda(\bar{\Lambda}) + \pi^-(\pi^+),\ \text{Branch ratio } = (99.88 \pm 0.035)\% \tag{5}$$

$$\Omega^-(\bar{\Omega}^+) \rightarrow \Lambda(\bar{\Lambda}) + \mathrm{K}^-(\mathrm{K}^+),\ \text{Branch ratio } = (67.8 \pm 0.7)\% \tag{6}$$

The mean of ionization energy loss, $\langle \mathrm{dE/dx} \rangle$, measured by TPC is used for identification of the charged daughter particles, π, K and p. Although the measured $\langle \mathrm{dE/dx} \rangle$ for a track has finite resolution due to the limited number of hit points measured by TPC, the central values of the measured $\langle \mathrm{dE/dx} \rangle$ for a particular particle species, as a function of momentum, can be effectively characterized by the Bichsel function. Hence a normalized $\langle \mathrm{dE/dx} \rangle$, $\mathrm{n}\sigma_{\mathrm{particle}}$, is used in particle identification. It is defined by

$$n\sigma_{\mathrm{particle}} = \frac{1}{\sigma_{\mathrm{particle}}} \log \frac{\langle \mathrm{dE/dx} \rangle_{\mathrm{measured}}}{\langle \mathrm{dE/dx} \rangle^{\mathrm{Bichsel}}_{\mathrm{particle}}} \tag{7}$$

where $\langle dE/dx \rangle^{\mathrm{Bichsel}}_{\mathrm{particle}}$, is the expected $\langle \mathrm{dE/dx} \rangle$ from the Bichsel function for a certain particle species at a given momentum and $\mathrm{n}\sigma_{\mathrm{particle}}$ is the $\langle \mathrm{dE/dx} \rangle$ resolution of the TPC at the same momentum for same particle species. The $\sigma_{\mathrm{particle}}$ distribution is approximately gaussian at a given momentum and is calibrated to be centred at zero with a width of unity for each particle species. A loose cut of $|n\sigma_{\mathrm{particle}}| < 4$ is used to select the charged daughter particles for the reconstruction of $\mathrm{K^0_S}$, $\Lambda(\bar{\Lambda})$, $\Xi^-(\bar{\Xi}^+)$ but a slightly tighter cut of $|n\sigma_{\mathrm{particle}}| < 3$ is used for selecting the protons in Ω^- $(\bar{\Omega}^+)$ reconstruction.

In order to improve the average momentum and energy-loss resolution, the charged daughter particle tracks were required to consist of at least 15 TPC hit points for the reconstruction of $\mathrm{K^0_S}$, $\Lambda(\bar{\Lambda})$, $\Xi^-(\bar{\Xi}^+)$ and Ω^- $(\bar{\Omega}^+)$. The $\mathrm{p_T}$ of daughter particles is required to be larger than 0.10 GeV/c for K^0_S, $\Lambda(\bar{\Lambda})$, $\Xi^-(\bar{\Xi}^+)$ and larger than 0.15 GeV/c for Ω^- $(\bar{\Omega}^+)$ reconstruction.

The weakly decaying strange hadrons, $\mathrm{K^0_S}$, $\Lambda(\bar{\Lambda})$, $\Xi^-(\bar{\Xi}^+)$, and Ω^- $(\bar{\Omega}^+)$, have a decay length of approx. 2–7 cm. Their decay topology can be reconstructed well with their daughter particle tracks measured by the TPC. Therefore, a certain set of

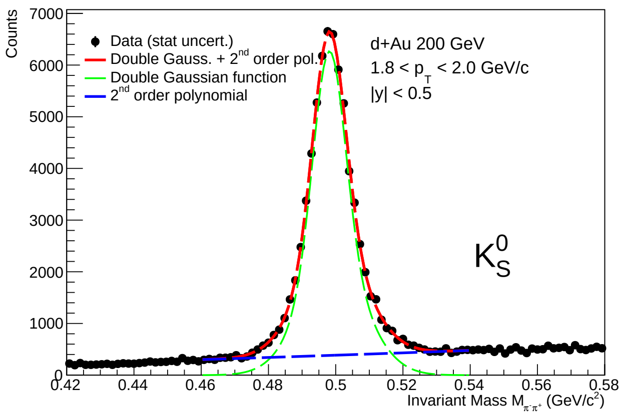

Fig. 2. K_s^0 invariant mass distributions at mid-rapidity (|y| $<$ 0.5), for the p_T bin of [1.8,2.0] GeV/c, for the most central 0-20% d+Au collisions at $\sqrt{s_{NN}}$ = 200 GeV. The distribution is fitted with double gaussian (for signal peak) plus polynomial functions (for background), shown as the red line. The horizontal blue dashed line represents the background.

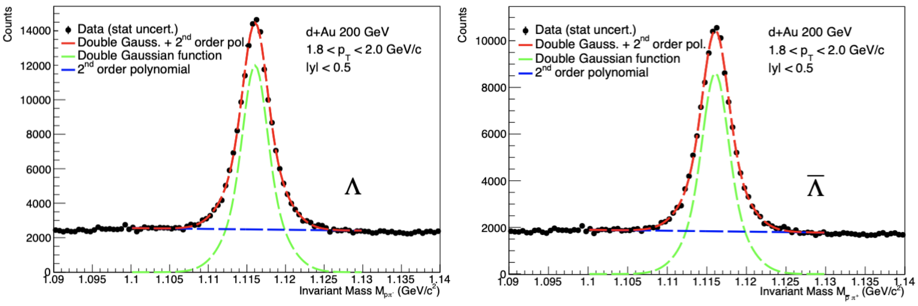

Fig. 3. Λ (left) and $\bar{\Lambda}$ (right) invariant mass distributions at mid-rapidity (|y| $<$ 0.5), for the p_T bin of [1.8,2.0] GeV/c, for the most central 0-20% d+Au collisions at $\sqrt{s_{NN}}$ = 200 GeV. The distribution is fitted with double gaussian (for signal peak) plus polynomial functions (for background), shown as the red line. The horizontal blue dashed line represents the background.

cuts can be applied to the topological variables in order to significantly reduce the combinatorial background. Such variables include the distance of closest approach (DCA) between the two daughter tracks, the DCA of the daughter tracks to the primary vertex, the DCA of the projected strange hadron path to the primary vertex, the decay length of strange hadrons, and the angles between the spatial vector pointing from the production vertex to the decay vertex and the momentum vector of strange hadrons. These cuts were optimized as a compromise between background reduction and signal efficiency.

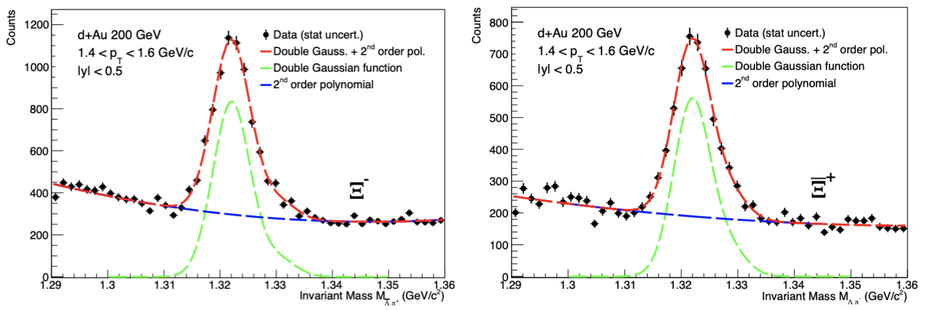

Fig. 4. Ξ^- (left) and $\bar{\Xi}^+$ (right) invariant mass distributions at mid-rapidity (|y| $<$ 0.5), for the p_T bin of [1.4,1.6] GeV/c, for the most central 0-20% d+Au collisions at $\sqrt{s_{NN}}$ = 200 GeV. The distribution is fitted with double gaussian (for signal peak) plus polynomial functions (for background), shown as the red line. The horizontal blue dashed line represents the background.

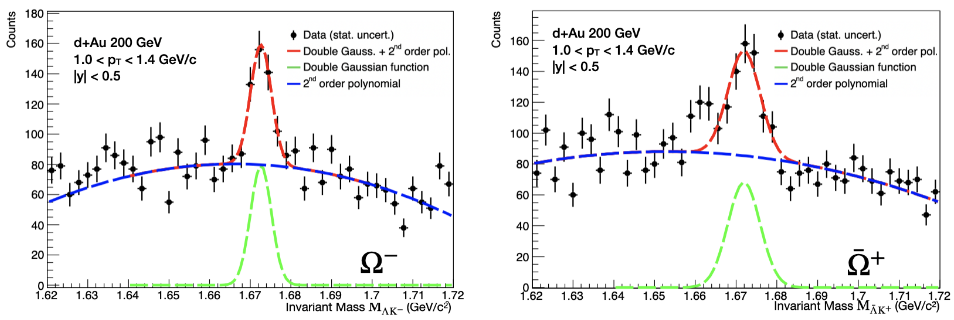

Fig. 5. Ω^- (left) and $\bar{\Omega}^+$ (right) invariant mass distributions at mid-rapidity (|y| $<$ 0.5), for the p_T bin of [1.0,1.4] GeV/c, for the most central 0-20% d+Au collisions at $\sqrt{s_{NN}}$ = 200 GeV. The distribution is fitted with double gaussian (for signal peak) plus polynomial functions (for background), shown as the red line. The horizontal blue dashed line represents the background.

We used double Gaussian and second order polynomial function to describe the signal and background, respectively. Raw yield is determined by using the bin counting method under the mass window of $M_0 \pm 3\sigma$, where M_0 is mass of K^0_S, Λ, Ξ or Ω and σ is the fitted width.

Invariant mass distributions for K^0_S, $\Lambda(\bar{\Lambda})$, $\Xi^-(\bar{\Xi}^+)$ and Ω^- $(\bar{\Omega}^+)$ are shown in Fig. [2], [3],[4] and [5] respectively. Raw yield is extracted for different p_T intervals and this raw yield is corrected for efficiency and acceptance to get corrected transverse momentum spectra for each particle.

4. Summary and Outlook

We presented invariant mass distribution of $\rm K^0_S$, $\Lambda(\bar{\Lambda})$, $\Xi(\bar{\Xi})$, $\Omega(\bar{\Omega})$ at mid-rapidity ($|\rm y| < 0.5$) in d+Au collisions at $\sqrt{s_{\rm NN}} = 200$ GeV. We are working on efficiency corrections for the corrected transverse momentum spectra to obtain integrated yield (dN/dy) and mean transverse mometum ($\langle p_T \rangle$). We are also working on nuclear modification factor ($\rm R_{dAu}$) and rapidity asymmtery ($\rm Y_{Asym}$) extraction of these strange particles to study nuclear effects.

5. Acknowledgement

The author acknowledges the support from the project grant No. SR/MF/PS-02/2021- PU.

References

1. K. H. Ackermann et al. (STAR Collaboration) Nucl. Instrum. Methods A **499**, 624 (2003).
2. G. Agakishiev et al. (STAR Collaboration) Phys. Rev. Lett. **108**, 072301 (2012).
3. J. Adams et al. (STAR Collaboration) Phys. Lett. B **637**, 161-169 (2006).
4. B. I. Abelev et al. (STAR Collaboration) Phys. Rev. C **76**, 054903 (2007).
5. B. I. Abelev et al. (STAR Collaboration) Phys. Rev. C **75**, 064901 (2007).
6. B. I. Abelev et al. (STAR Collaboration) Phys. Rev. C **79**, 034909 (2009).
7. B. I. Abelev et al. (STAR Collaboration) Phys.Lett.B **616**, 8-16 (2008).